PRJ, Vol. 5 (January 1993); P. 37–45, 14 FIGS, 1 TABLE.

AMPLITUDE FEATURES OF FAST COMPRESSIONAL WAVES IN POROUS MEDIA ON ZERO-OFFSET SYNTHETIC SEISMOGRAMS

A.A.A. Othman*

مظاهر سعات الموجات التضاغطية السريعة في الأوساط المسامية على السيسموجرامات التخليقية صفرية الإزاحة

عادل علي علي عثمان

تتأثر سعة الموجات السيزمية بنوع الوسط التي تمر خلاله. لذلك صمم نموذج جيولوجي لدراسة التغير في سعات الموجات السيزمية داخل عدة صخور لها درجات مسامية مختلفة. تم إختيار أربعة أنواع من الصخور لتوضيح مظاهر اختلاف السعات وذلك باستخدام السيسموجرامات التخليقية.

ABSTRACT

The seismic amplitudes are clearly affected by the type of medium through which waves are propagated. A geologic model was designed to study the changes in amplitudes of the seismic waves within several rocks of different porosities. Four rocks are selected to show these features using synthetic seismograms.

INTRODUCTION

The amplitude of seismic waves decay by one of several processes like scattering, geometrical spreading, reflections, transmissions, dispersion or intrinsic dissipation. The intrinsic dissipation is present when the medium is anelastic. The present study considers the medium as elastic, homogeneous, and isotropic. Fluid-mineral chemical interactions and the microcracks were not studied.

Geophysicists, in the sixties, became interested in using the amplitude of the reflected events as a direct method to the presence of hydrocarbons (Domenico, 1974). Until 1970, only the variations in the amplitude of the reflected signal were used as a qualitative tool for identifying seismic events. A quantitative analysis of the character of reflected signal might lead to more information of some of the acoustical properties of the rock formations (Sheriff, 1974).

The velocity of seismic waves that travel through porous media depends not only on the rock matrix velocity, but also on the porosity and the characteristics of the interstitial fluids. Amplitudes of reflected seismic waves are important evidence of the anomalous effect of interstitial fluids (water and/or hydrocarbons). This depends on the reflection coefficients of the interfaces, separating different lithologies in a sequence. The polarity of the reflected seismic pulse can help to identify a saturated reservoir interface (Sheriff, 1974). Phase reversal occurs if the reflectivity changes sign.

Bright spots became the hottest topic in exploration, and with good reason, because they were effective in pointing gas reservoirs in the Gulf of Mexico and other areas with similar geologic characteristics. Observations of time sections, led to false synclinical structures corresponding to reflections from below the gas horizons (Hammond, 1975). Some characteristics of the time signal is expected to show certain typical changes over the region containing gas, oil or other fluids.

Quantitative estimations are presented here to discuss some of the above mentioned parameters, taking in consideration that the computations are carried out for the zero-offset case.

*University of Qatar, Geology Dept, P.O. Box 2713, Doha, Qatar

THEORY

Exploration geophysicists are interested in the lithology, porosity, permeability, saturation and type of pore fluid of the subsurface formations. Therefore, there are many authors, who tried to relate the propagated wave velocity to rock parameters. The time average equation (Wyllie et al., 1962) empirically relates velocity and formation parameters for wide range of porosity as:

$$v=\{(\phi/v_f)+(1-\phi)/v_m\}^{-1} \quad (1)$$

where ϕ is porosity, v is liquid saturated rock velocity, v_f is pore fluid velocity, v_m is matrix velocity (massive rock).

The time average equation (1) displays the relationship between velocity and porosity which, according to Gardner and Harris, 1968, can be used for shallow porous layers. This equation cannot be applied for gas-saturated materials. Therefore, a modification for the equation is needed. In case of gas-saturated reservoirs, the modified Wyllie equation (Wyllie et al, 1962), would take the following new form (Marschall, 1984):

$$v=\{(\phi s_w/v_w)+[\phi(1-s_w)/(v_g \log(c_g/c_m))] +(1-\phi)/v_m\}^{-1} \quad (2)$$

here v is the wave velocity in a gas and fluid saturated porous medium, v_w is the wave velocity in water, v_g is the wave velocity in gas. S_w is the water saturation fraction, c_g is gas compressibility, c_m is matrix compressibility. The compressibility ratio of the fluids (gas) with respect to solids is nearly equal to 10 (Marschall, 1984) and in equation (2), the logarithm of this ratio will equal one.

Synthetic seismograms $S(t)$ can be computed from the convolution of the source wavelet $W(t)$ with reflectivity $R(t)$. It may be expressed as:

$$S(t)=R(t)*W(t) \quad (3)$$

The asterisk denotes convolution. The reflection coefficient R is computed from the equation:

$$R=(\rho_{i+1}v_{i+1}-\rho_i v_i)/(\rho_{i+1}v_{i+1}+\rho_i v_i) \quad (4)$$

where i denotes the i-th layer and

$$\rho=\rho_f+(1-\phi)\rho_m \quad (5)$$

where ρ is density, ρ_f is fluid density, ρ_m is matrix density.

Using the modified equation (2), a great number of synthetic traces may be computed, for each of which the suitable reservoir parameters have been modified. This set of traces may be used as a guide line for subsequent interpretation of the actual seismic data, after having applied the appropriate frequency-band limitation in form of the input source wavelet.

THE GEOLOGICAL MODEL

The geological model that has been chosen for investigation is shown in Fig. 1. It consists of three layers (A, B and C). Layers A and C are non-porous shale. Layer B is selected to be either dolomite, limestone or sandstone. The acoustical parameters of the model (slow p-wave and s-wave are neglected) are given in Table 1.

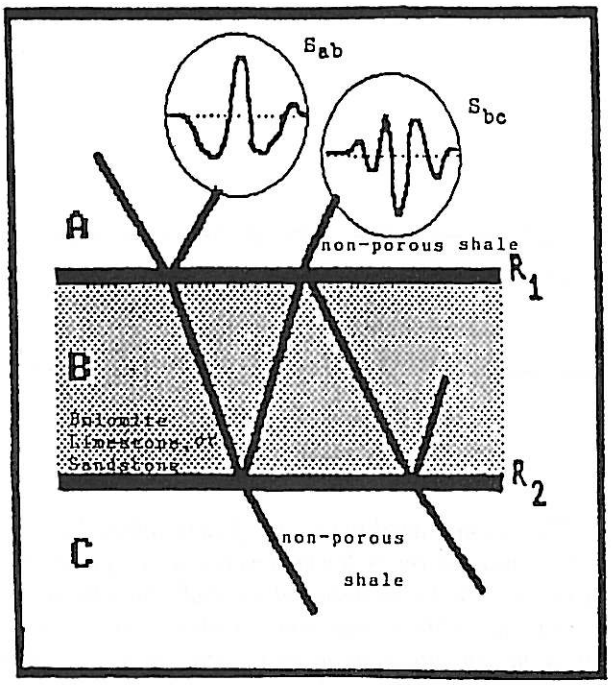


FIG. 1. A three geologic layers model A, B and C with reflection coefficients R_1 and R_2. S_{ab} and S_{bc} denote two reflected signals from the upper and lower interfaces of layer B.

Table 1. Numerical Parameters Used in the Studied Model

	Velocity (m/s)	Density (g/cc)	Porosity (%)
Layer A:			
Shale	4500	2.60	0
Layer B:			
Dolomite	7000	2.87	5 to 15
Limestone	6400	2.69	10 to 20
Sandstone	5500	2.65	15 to 35
Shale	4500	2.60	40 to 50
Layer C:			
Shale	4500	2.60	0
Fluids:			
Water	1500	1.00	—
Oil	1200	0.85	—
Gas	480	0.15	—

DESCRIPTION OF MODEL OUTPUTS

A simple calculation using the modified equation (2) was carried out to relate velocity with porosity over the given ranges in the studied geologic model (see Table 1). Fig. 2 shows the plots of all four rocks: shale, sandstone, limestone and dolomite at gas-, oil- or water-saturated cases. The wave velocity in dolomite highly decreases with increasing porosity and in gas-saturated case is lower than that in water-saturated one. This relation, for the indicated range, is almost linear in limestone, and the velocity of gaseous case is still lower than that of oil and of water saturated cases. A weak sensitivity appears in saturated sandstones. In shale, velocity is almost non-sensitive to porosity.

A computer program to execute the synthetic seismograms by inserting the porosity and follow its effects on amplitudes was generated by the author. A test was made in Fig. 3 to show the presence of porosity effects, if layer B was a shale flanked by the shale on the top as well as at the bottom. There are no reflection coefficients in the case of massive shale in layer B; i.e. the porosity is zero. According to the introduction of the porosity into layer B, a difference in velocity occured. A series of plots were computed for the dolomite, limestone and sandstone; in both gas- and oil-saturated cases. Every plot consists of three parts; each one contains many synthetic traces calculated over a given range of porosity for every rock type. In each part, a synthetic trace was calculated for a massive (non-porous) rock to consider it in the comparative studies when porosity is introduced into calculations.

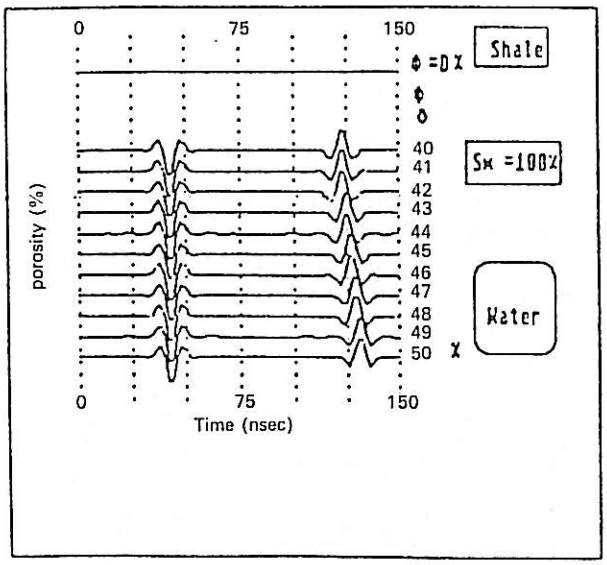


FIG. 3. Calculated synthetic seismograms in case of layer B is water saturated shale, for different porosity values.

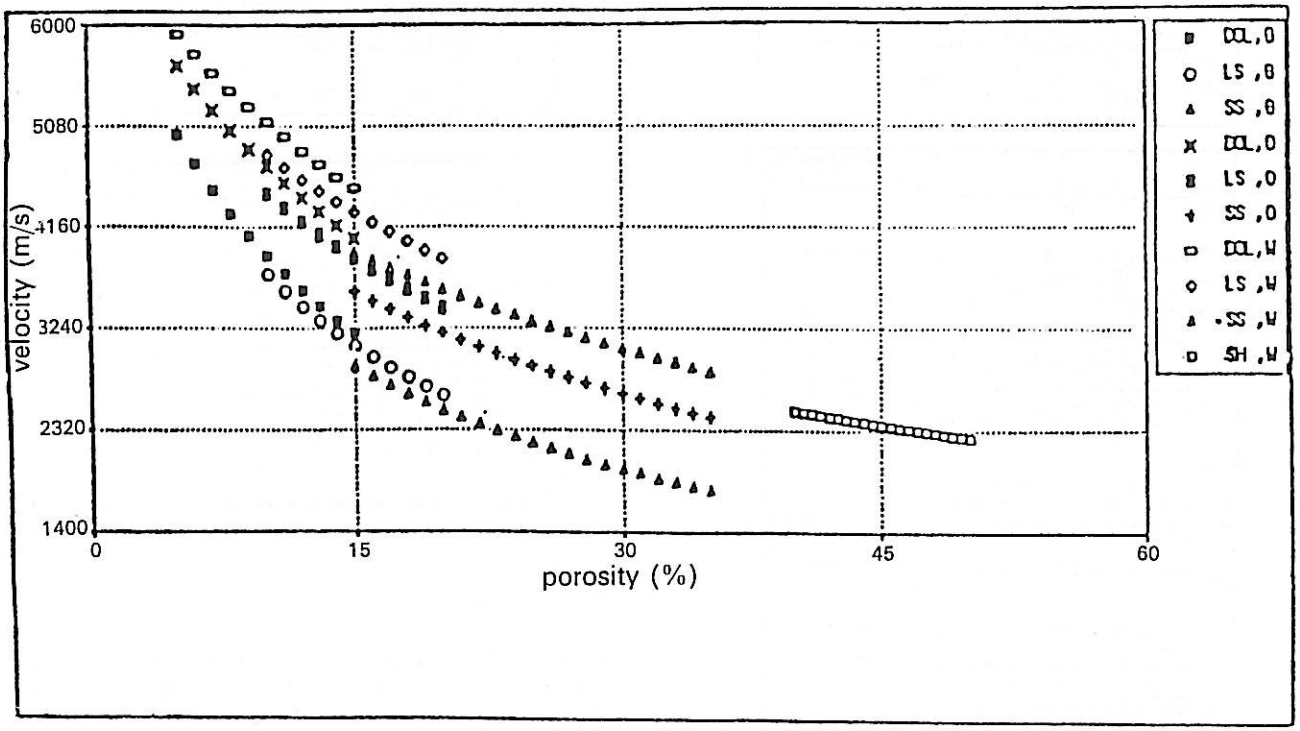


FIG. 2. Seismic velocity as function of porosity for limestone, dolomite, sandstone and shale in the studied model, in (G) gas-, (O) oil-, and (W) water-saturated medium.

SYNTHETIC SEISMOGRAMS IN GAS AND OIL SATURATED CASES

1. Dolomite

In a gas-saturated dolomite, the reflected event comes from the bottom of layer B (dolomite), with a

delay time compared with the massive case, which increases with increasing porosity. These time shifts are larger at higher porosity. Fig. 4A shows, also, a reverse of amplitude polarity starting at a porosity equal to 8%. At the mixed case (gas/water), this polarity reversal took place at a porosity value of 10%, as shown in Fig. 4B. Polarity reversals appear at a porosity of 15% in a water-saturated dolomite, as shown in Fig. 4C. Time shifts of the second event (the reflected from the bottom of layer B) generally decrease by increasing the water saturation percentage in the rock.

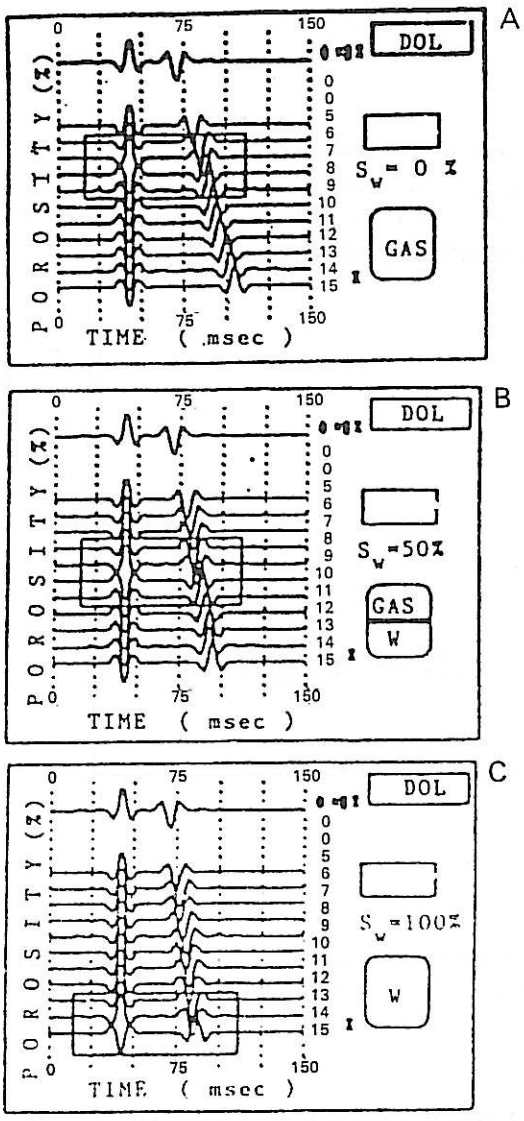


FIG. 4. Synthetic seismograms for partially gas-saturated dolomite, at different water saturations, calculated for layer B in the studied model.

Fig. 5A shows a case of oil saturated dolomite, in which the polarity reversals occur at a porosity equal to 12%. These reversals start at a porosity equal to 14% in the mixed (oil/water) case, see Fig. 5B. Polarity reversals at water-saturated case is

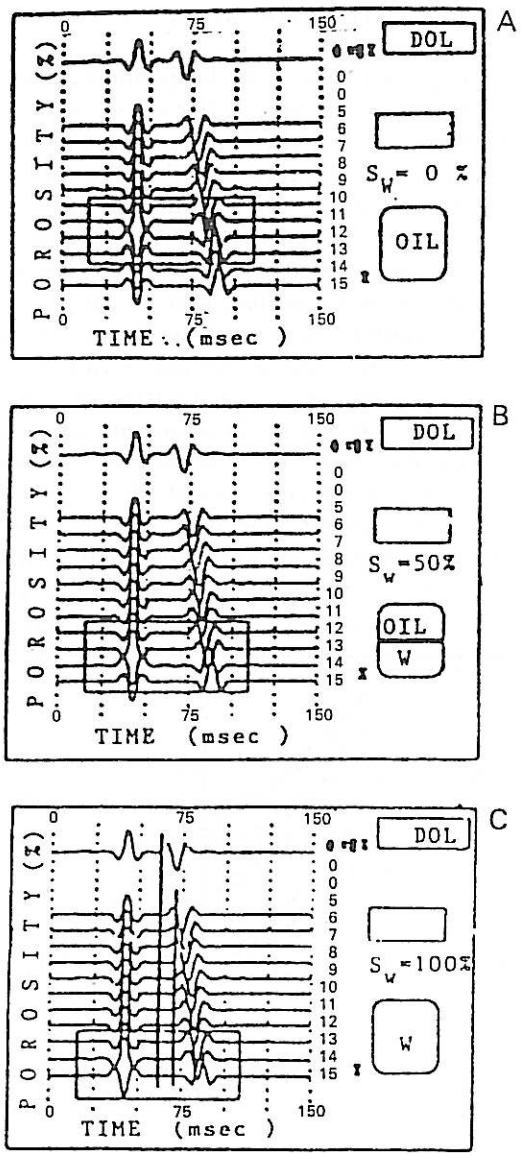


FIG. 5. Synthetic seismograms for partially oil saturated dolomite, at different water saturations, calculated for layer B in the studied model.

mentioned above and is shown in Fig. 5C. The delay shift is, in general, smaller than that in gas-saturated dolomite.

2. Limestone

Amplitude polarity changes sign with respect to a massive limestone, as seen in Fig. 6. Gas-saturated rocks give large transient times for the second event with increasing porosity fractions, see Fig. 6A. These time shifts are smaller in the gas-water mixture case as shown in Fig. 6B. Water-saturated limestone displays a case of polarity reversals starting at lower values of the proposed porosity range as shown in Fig. 6C.

For oil saturated limestones, time delays are the only difference with respect to the gas saturated case.

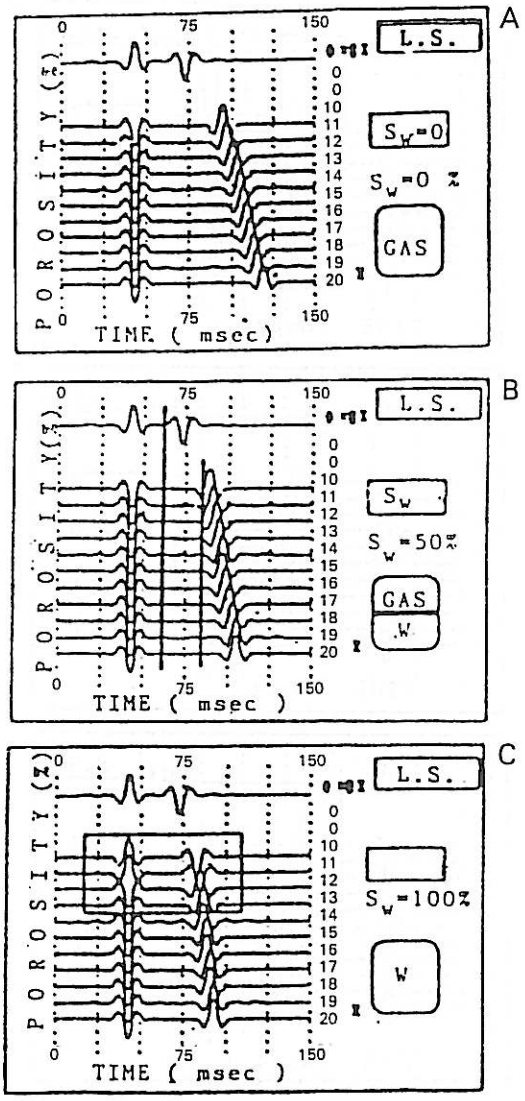


FIG. 6. Synthetic seismograms for partially gas-saturated limestone, at different water saturations, calculated for layer B in the studied model.

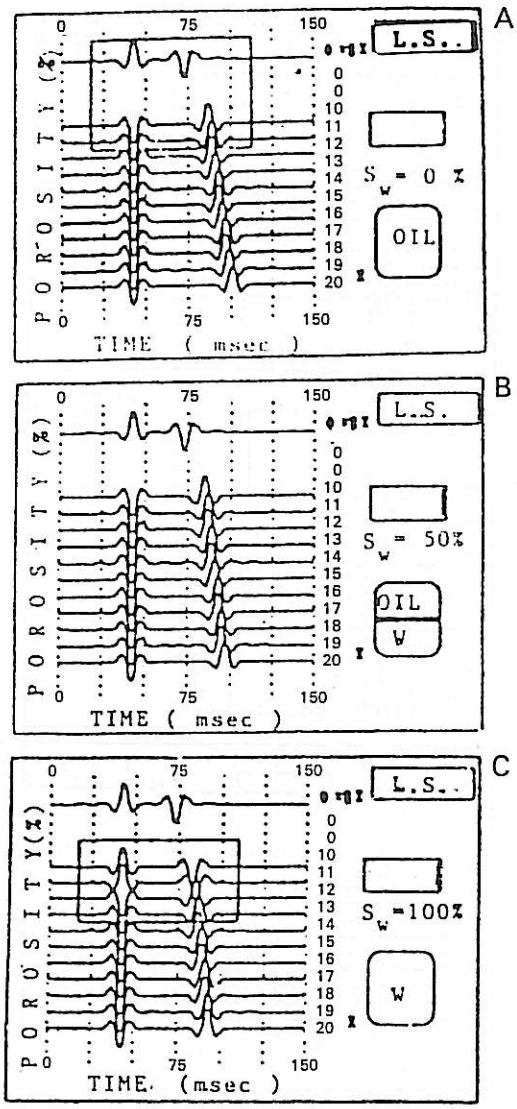


FIG. 7. Synthetic seismograms for partially oil-saturated limestone, at different water saturations, calculated for layer B in the studied model.

These delays are smaller than in gas saturation, as indicated in Fig. 7A. Introduction of water in the model decreases the time shift as shown in Fig. 7B. This is clearly shown in the case of water saturated limestone as seen in Fig. 7C. Reverse of amplitude polarity appears at porosity equal to 12%.

3. Sandstone

A porous sandstone is highly affected by the presence of pore fluids. Some features are observed in Fig. 8A, for the gas-saturated case. Time shifts increased at higher porosity fractions, but once the water is introduced, these time shifts decreased, as shown in Fig. 8B and Fig. 8C.

For oil-saturated sandstone rocks polarity reversals are present all over the porosity range as well as gas saturated case. The observable difference is a decrease of time shifts referring to massive sandstones with respect to gas-saturated one, as displayed in Fig. 9a.

Fig. 9B and Fig. 9C exhibit decrease in time shifts when the percentage of water saturation is increased.

AMPLITUDE CHARACTERISTICS DUE TO LAYER B

The following discussion is restricted to study the forms of the events reflected from the bottom of layer B.

Amplitudes in a porous dolomite have different features over the selected porosity range, at different degrees of water saturation. Fig. 10 shows the effects of three different cases of saturations on the amplitude. A quick comparison between the three cases confirm that in gas-saturated dolomite, the amplitudes are higher (bright spots). The calculated

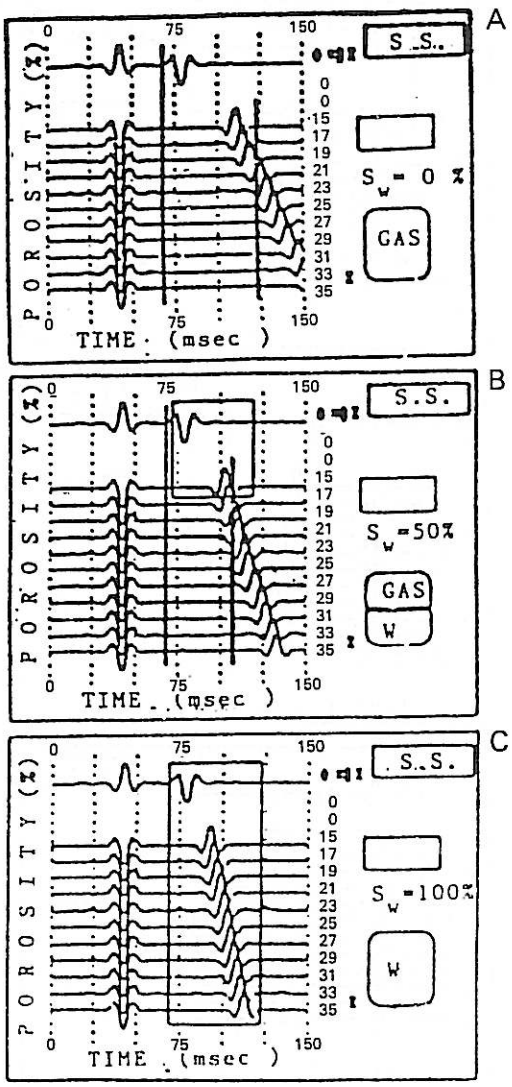


FIG. 8. Synthetic seismograms for partially gas-saturated sandstone, at different water saturations, calculated for layer B in the studied model.

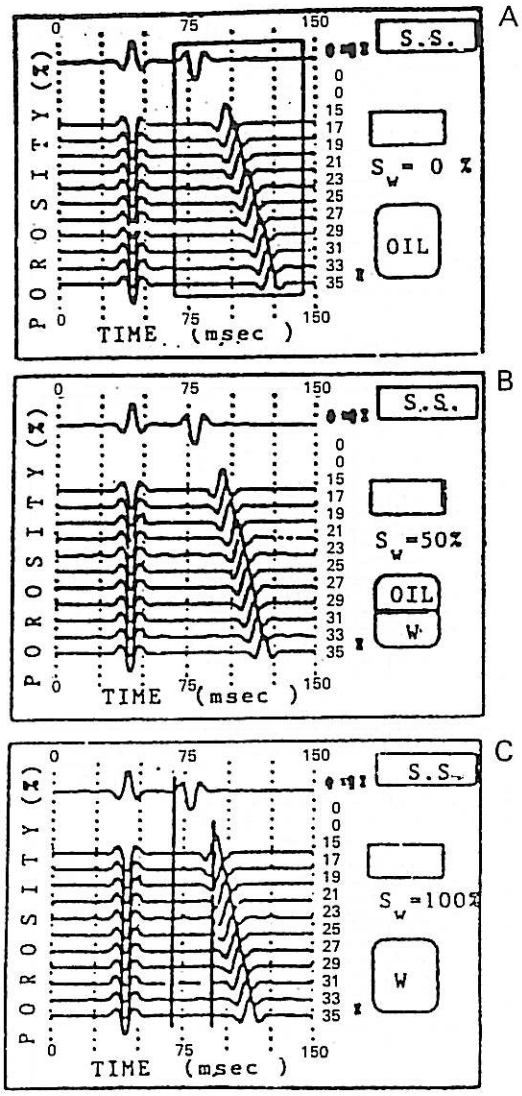


FIG. 9. Synthetic seismograms for partially oil-saturated sandstone, at different water saturations, calculated for layer B in the studied model.

amplitudes show an increase with increasing the porosity values. The presence of water in the formation decreases the amplitudes of seismic events, and moves the upper curve downwards. Before and after intersecting the zero-marked line (solid line), the amplitudes show changes from negative to positive values; i.e. polarity reversals. These reversals start at porosity higher than 6% (for $S_w=0\%$), and higher than 8.25% (for $S_w=50\%$).

Oil-saturation decreases the amplitude lower than that of gas saturated rock. Polarity of amplitudes changes signs at porosity higher than 11.75%. Due to presence of water, the last value will be shifted to porosity higher than 13.25%. If layer B is water saturated dolomite, amplitudes of travelling events increase with increasing porosity. A reverse polarity appears at porosity higher than 12.5%. The amplitudes of the water saturated case are generally larger than that of oil mixded with water. At porosity equals to 8.25%, seismic waves were reflected with the same amplitude, in both oil- and water- saturated cases, as observed in Fig. 10.

This situation is different in porous limestone as observed in Fig. 11. Acoustic waves that travel through a gas-saturated limestone have larger amplitudes which have change polarity upon reflecting at the bottom of layer B. The only exception is for $S_w=100\%$ for porosity values less than about 10.5%. Gas amplitude decreases downwards as water saturation is increased to 50%, (Fig. 11). A similar condition was observed in the case of oil-saturated rock, where the amplitudes were decreased by increasing S_w.

Amplitudes of travelling waves through gas saturated sandstone have a non linear relation with porosity, as shown in Fig. 12. The increase is steady for porosities less than 25%, and takes a linear shape for higher porosities. If the water saturation

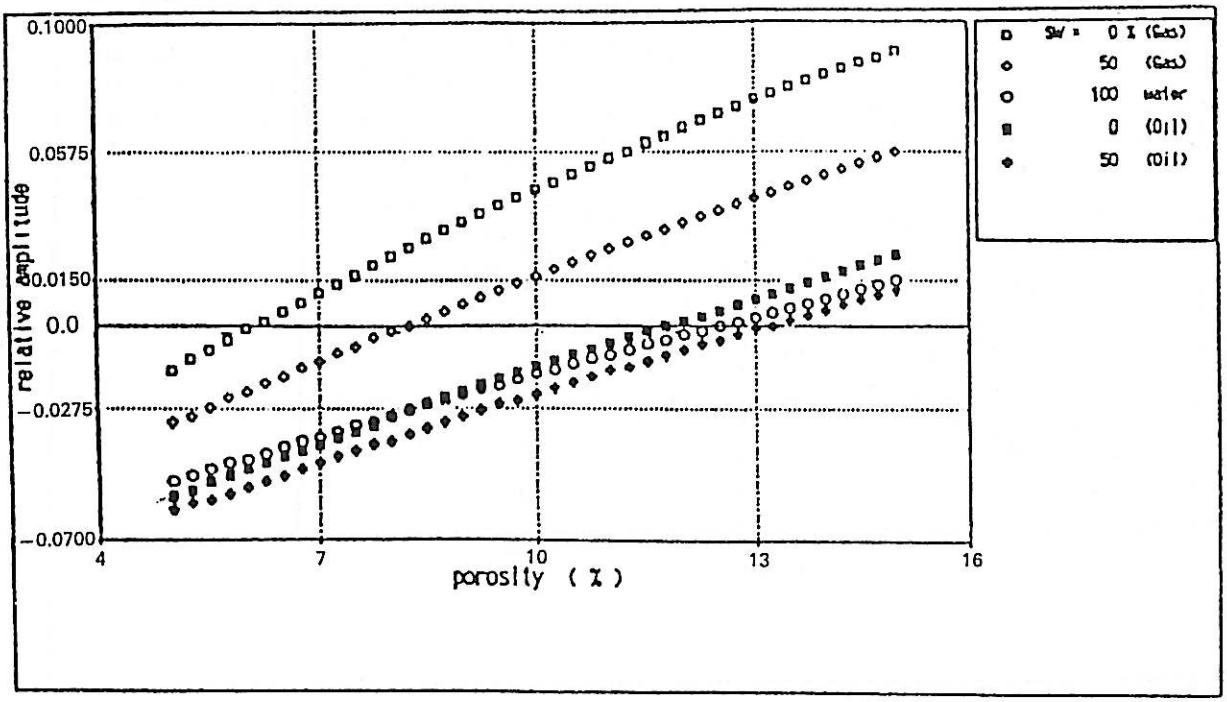


FIG. 10. Seismic amplitude and porosity for S_w=0%, 50% and 100% in both gas- and oil-filling porous dolomite.

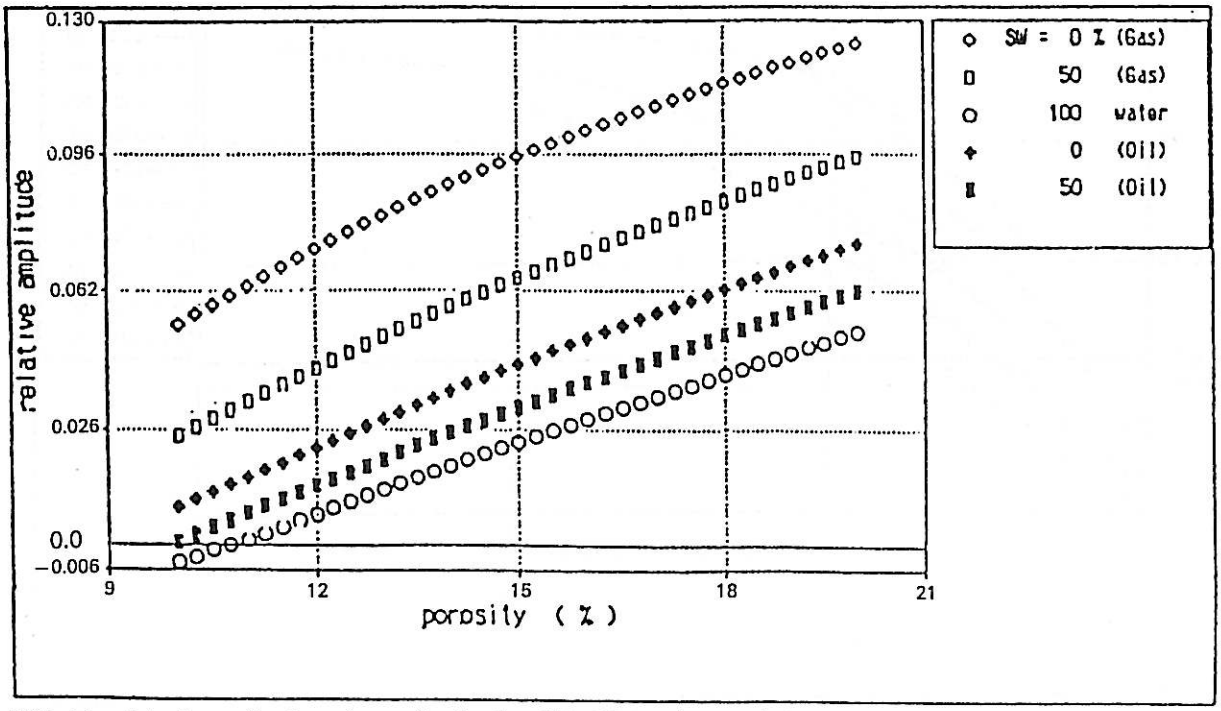


FIG. 11. Seismic amplitude and porosity for S_w=0%, 50% and 100% in both gas- and oil-filling porous limestone.

increases, it decreases the gas amplitudes. Oil saturated amplitudes decrease with increasing water content in the pores, as shown in Fig. 12. Water-saturated sandstones show amplitudes of minimum values and of linear nature with increasing porosity. There are no polarity reversals detected as seen in Fig. 12.

A complete picture was created in Fig. 13. Amplitudes of the waves passing through all the four rocks are displayed together. Polarity reversals take place at porosities starting from 7.5% to 15%. Sandstones have higher gas-saturated amplitudes than other studied rocks in the present work. Shales have also large amplitudes at higher porosities.

FIELD DATA

Three measured field records were collected from different published works to declare the above discussed ideas. These examples include bright spot

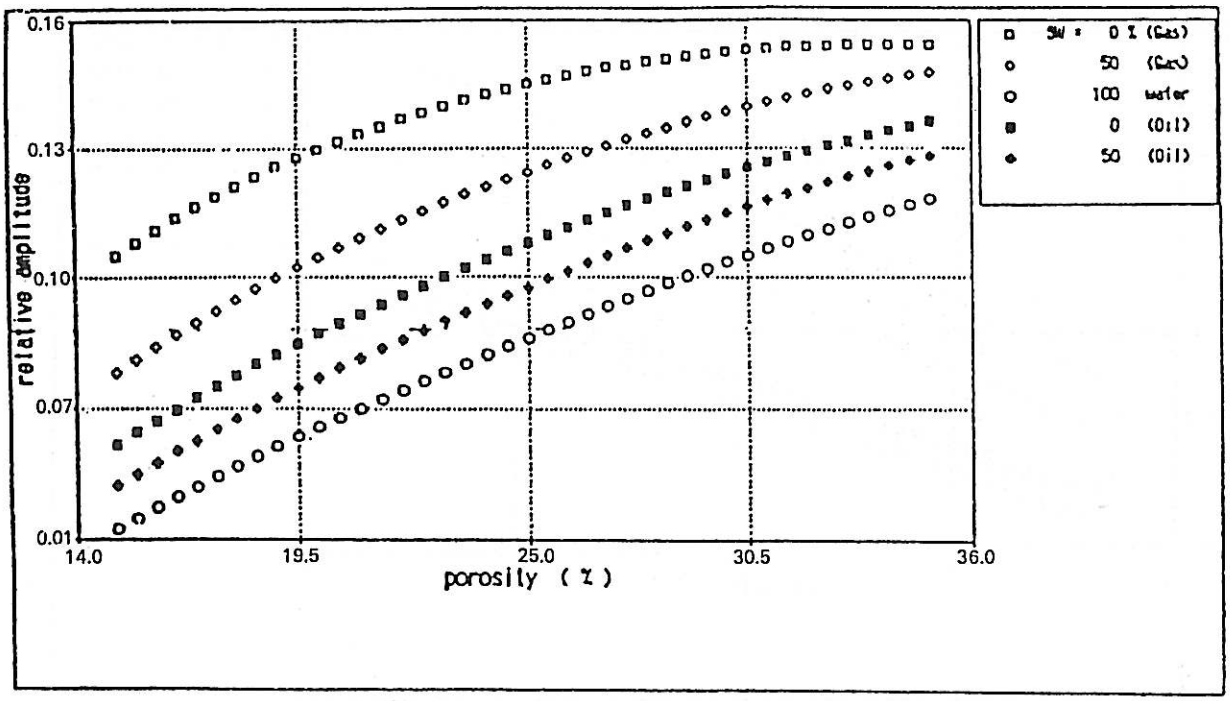


FIG. 12. Seismic amplitude and porosity for S_w=0%, 50% and 100% in both gas- and oil- filling porous sandstone.

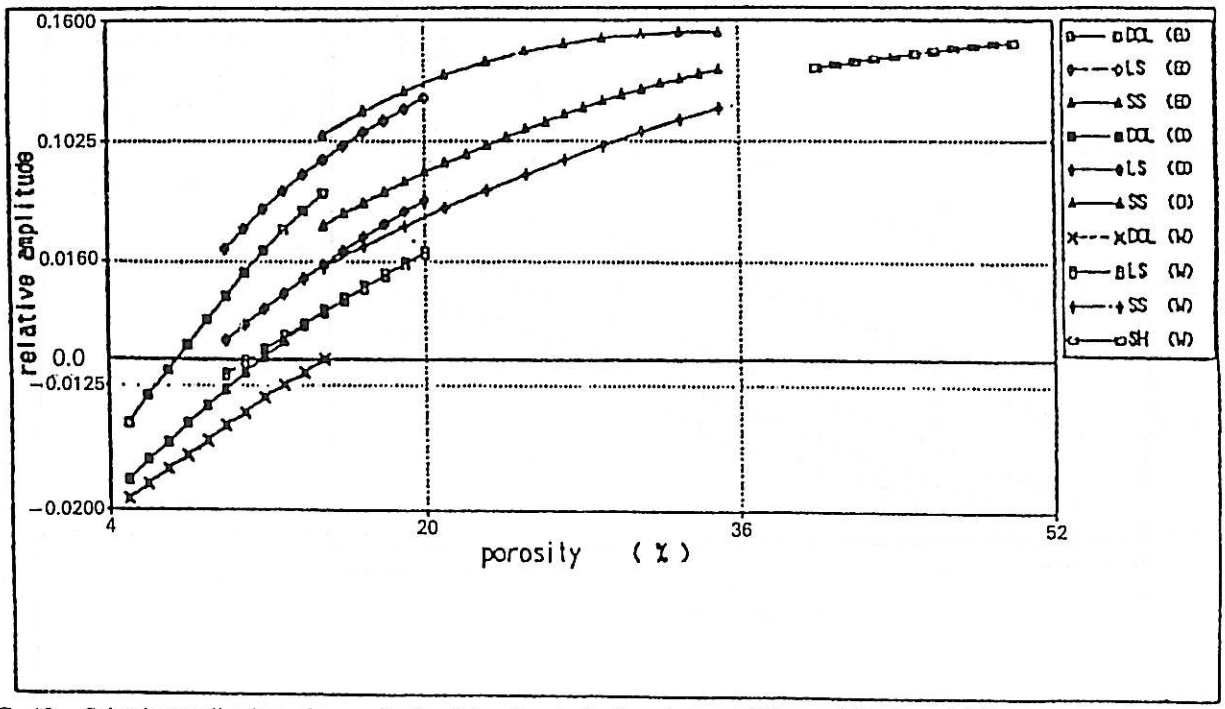


FIG. 13. Seismic amplitude and porosity for dolomite, shale, limestone; at (G) gas- (O) oil- and (W) water- saturated cases of the received second event in the studied model.

amplitudes, which help in the detection of gas reservoirs. Fig. 14A and Fig. 14B show gas fields. Amplitudes are higher than the adjacent horizons, which describe clearly the bright spots, giving to a similar amplitude characteristic like that calculated in the studied model. In Fig. 14B, a drilled well is indicated on the seismic line. Well information is tied with the presented time section, and the black markers are sandstones. Gas saturated sandstone, as mentioned in the previous section, gives higher amplitudes (bright spots).

In Fig. 14C, the two boxes display the polarity reversals which may be interpreted as structural changes (i.e., fault) or as a difference in the pore fluid contents, as observed from the calculated results of the studied model.

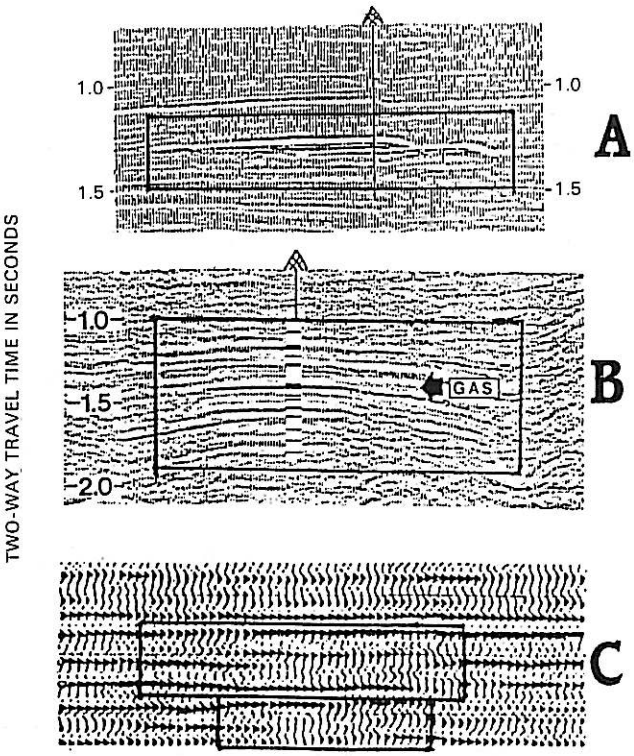


FIG. 14. Field seismic time sections describe the bright spots and polarity reversals signals.

CONCLUSION

The present study deals with travelled amplitudes in porous media. It is carried out through calculations of a designed model. The following conclusions can be considered:

1. Amplitudes of travelled waves in porous media are highly affected by porosity, the type of fluid (gas, oil, water) and the amount of fluid (porosity, saturation). Addition of water in the pores decreases these amplitudes.

2. In dolomite and limestone polarity reversals appear if the varying porosity crosses a specific value.

REFERENCES

Domenico, S.N., 1974, Effect of Water Saturation on Seismic Reflectivity of Sand Reservoirs Encased in Shale, Geophysics, vol. 39, pp. v 759–769.

Gardner, G.H.F., and M.H. Harris, 1968, Velocity and Attenuation of Elastic Waves in Sands, 9th Ann. Logging Symposium, Trans, (SPWLA), pp. M1-M19.

Hammond, A.L., 1975, Bright Spots: Better Seismological Indicators of Gas and Oil, Oil Commentary, vol. 12, pp. 2.

Marschall, R. 1984, Some Aspects of Deconvolution, Preprint, CDC's Petroleum Seminar, Geneva, Switzerland.

Sheriff, R., 1974, Seismic Detection of Hydrocarbons; the Underlying Physical Principles, Preprint, VI Annual Offshore Technology Conference, Houston, Texas.

Wyllie, R.J., Gardner and A.R. Gregory, 1962, Studies of Elastic Wave Attenuation in Porous Media, Geophysics, vol. 27, pp. 569–589; and discussion (1963): Geophysics, vol. 28, pp. 1074.